(*The 41st International Workshop on Water Waves and Floating Bodies, 26-29 April, 2026, Plitvice, Croatia*)

Coupled responses between a ship and recessed moonpools

Junxuan Chen*, Zhiliang Lin, Xinshu Zhang†

State Key Laboratory of Ocean Engineering, Shanghai Jiao Tong University, Shanghai 200240, China

Highlights

- Extensive experimental investigations were conducted to examine the coupled hydrodynamic behavior of a ship with a recessed moonpool under both regular wave and white-noise irregular wave conditions.
- The results indicate that increasing the recess length reduces the influence of piston-mode resonance on heave motion, while enhancing its impact on surge motion in head-wave conditions.

1 Introduction

A moonpool is a vertical opening in a ship or offshore platform. When the frequency of the incoming waves approaches the natural frequency of the moonpool, the free-surface response inside the moonpool can be greatly amplified, potentially causing slamming and green-water events. Accurate prediction of the natural frequencies of moonpool resonance, including both piston and sloshing modes, is essential. Many studies have focused on estimating these natural frequencies for two-dimensional and three-dimensional moonpools without recesses.(Molin, 2001; Molin *et al.*, 2018; Zhang *et al.*, 2019).

Recent moonpool designs incorporate recessed structures to facilitate the installation of subsea equipment. Molin (2017) developed a new model to evaluate the natural frequencies of the recessed moonpool. Zhang & Li (2022) proposed semi-analytical models to compute the natural frequencies and modal shapes for three-dimensional moonpools both with and without recesses in finite water depth. To examine the coupled dynamics between a ship and moonpools of varying sizes, Senthuran *et al.* (2020) performed experiments of a ship with clean moonpools (i.e., without recesses) of varying dimensions in an ocean wave basin.

Most of the previous studies have concentrated on clean moonpools, with relatively little attention paid to the coupled responses between a ship and a recessed moonpool. As a result, the influence of recessed moonpools on ship motions remains poorly understood. Zhang *et al.* (2026) examined the influence of recesses on the nonlinear free-surface response of a three-dimensional moonpool in a ship being in fix condition. Building upon this work, the present study seeks to further investigate the impact of recesses on the coupled dynamics between a ship and a recessed moonpool.

2 Experimental set-up

Experiments were conducted in the deepwater wave basin at Shanghai Jiao Tong University, which is 50 m long, 40 m wide and has a water depth of 8 m. The flap-type wavemakers are installed along two adjacent sides of

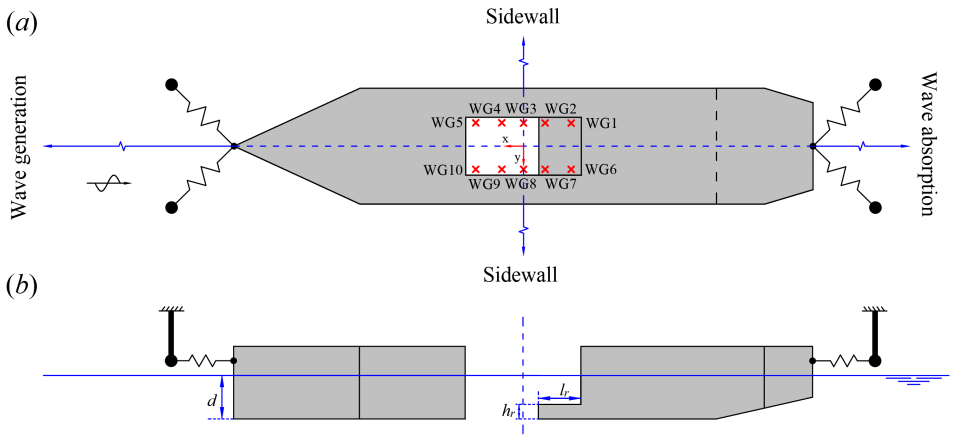

Figure 1: Sketch of the ship model with a recessed moonpool in the wave basin. Ten wave gauges are placed inside the moonpool. (*a*) Top view. (*b*) Side view.

*Presenting author
†xinshuz@sjtu.edu.cn

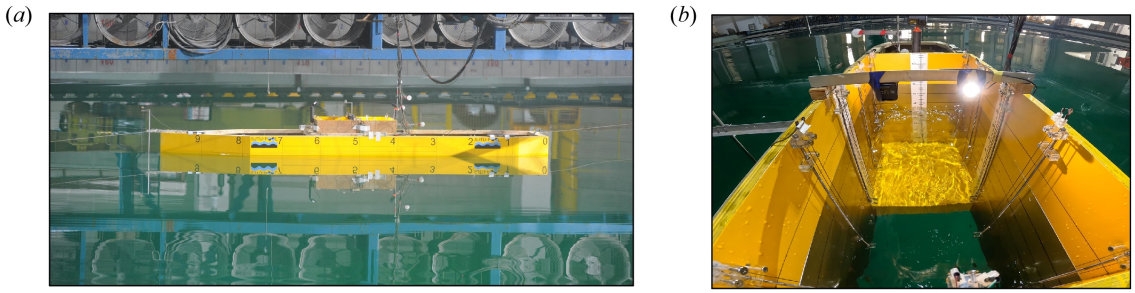

Figure 2: The ship model and the moonpool. (a) A snapshot of the ship model with a soft-mooring system; (b) A snapshot of video recordings of the moonpool response inside RMP4.

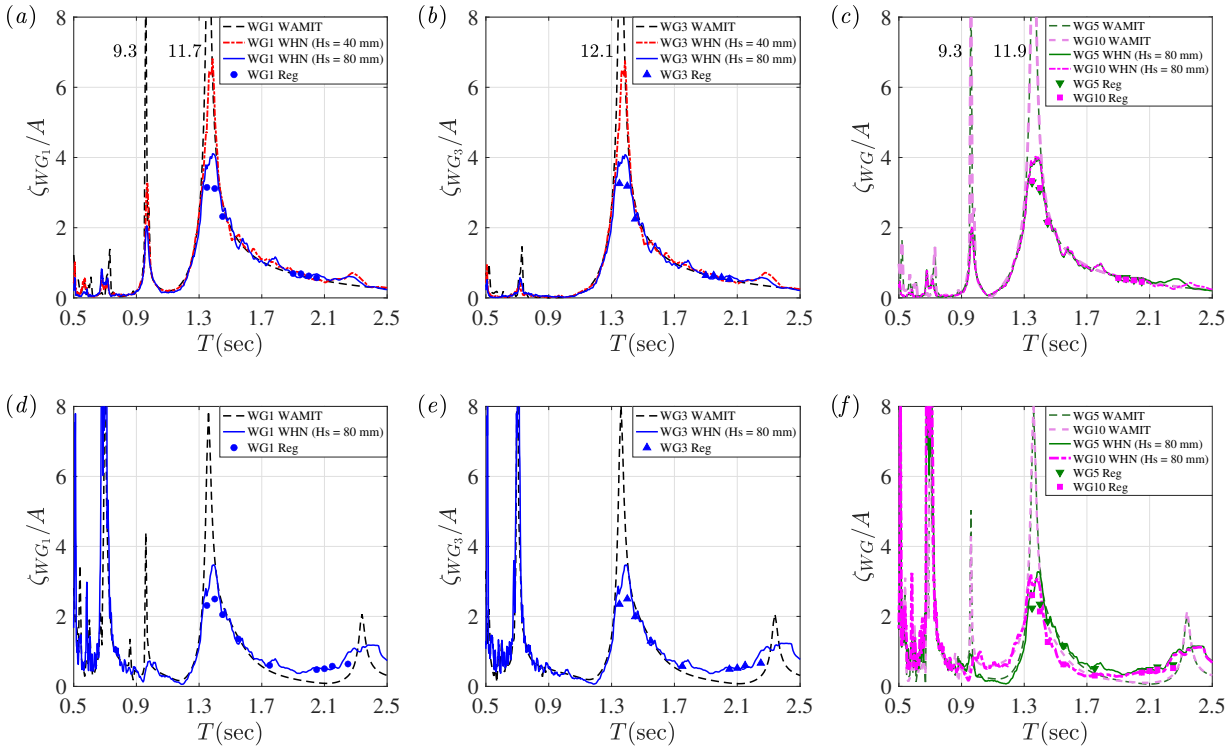

Figure 3: RMP0, free-surface elevation RAOs: (a) WG1, head wave; (b) WG3, head wave; (c) WG5 and WG10, head wave; (d) WG1, beam wave; (e) WG3, beam wave; (f) WG5 and WG10, beam wave. A and ζ denote the amplitudes of the incident wave and free-surface response, respectively.

the wave basin, while wave-absorbing beaches are located on the opposite sides to reduce wave reflections. In the present study, both the free-surface elevations inside the moonpool and the ship motions were measured.

The ship model measures 4 m in length, 0.8 m in width, and 0.3 m in draft, with a scale ratio of 1/40. As illustrated in Fig. 1, the coordinate system is centered at the middle of the moonpool on the horizontal plane. Ten wave gauges are installed inside the moonpool, five on each side. Four moonpools were tested: RMP0, RMP2, RMP3, and RMP4, corresponding to recess lengths of 0, 0.2, 0.3 and 0.4 m, respectively. A ship model without a moonpool (denoted as NMP) was also tested in the experiments.

Photos of the ship model along with a soft-mooring system, positioned at the center of the wave basin, are shown in Fig. 2. Two cameras were mounted above the moonpool to record videos of the flow inside the moonpool. The experiments were carried out under regular (Reg) waves of varying periods, maintaining a wave steepness of $H/\lambda = 1/80$, where H is the wave height and λ is the wavelength of the incident waves. Additionally, white-noise (WHN) irregular waves with significant wave heights of $H_s = 40\,\text{mm}$ and $H_s = 80\,\text{mm}$ were tested.

3 Results

The experimental results of the free-surface response inside the moonpool and ship motion are compared with those obtained using the wave diffraction/radiation code WAMIT. The natural periods of the moonpool were determined by analyzing the free-surface elevation RAO curves and modal shapes derived from the results of the white-noise tests.

Fig. 3 illustrates the free-surface responses at WG1, WG3, WG5, and WG10 (see Fig. 1 for locations) inside

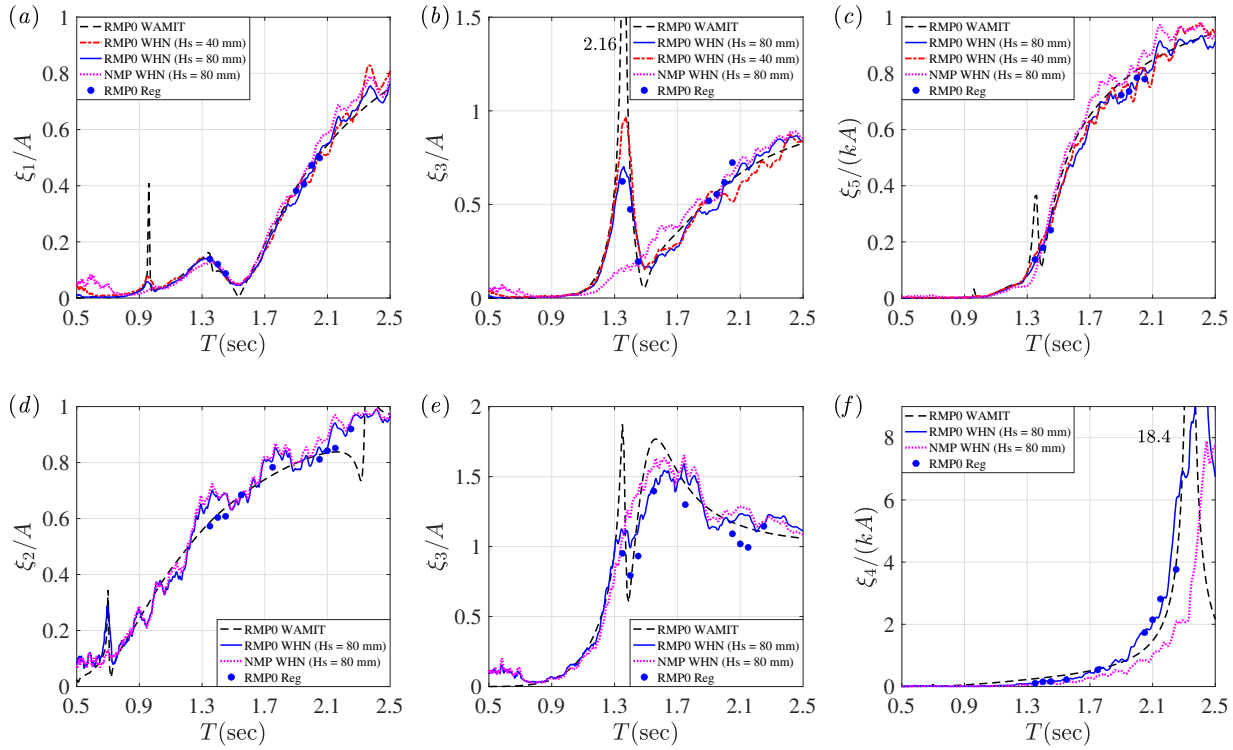

Figure 4: RMP0, motion response RAOs: (a) Surge, head wave; (b) Heave, head wave; (c) Pitch, head wave; (d) Sway, beam wave; (e) Heave, beam wave; (f) Roll, beam wave. ξ denotes the amplitude of the motion response.

RMP0 (without recesses) under head and beam wave conditions. The measurements at WG1 positioned above the recess are analyzed in detail. The results at WG3 are used to examine the response at the moonpool center, while the measurements at WG5 and WG10 are compared to assess the symmetry of the free-surface responses under head waves.

In general, the results of the regular wave tests are consistent with those of the white-noise tests with $H_s = 80$ mm. However, the free-surface RAO results of white-noise tests with $H_s = 40$ mm are higher than those with $H_s = 80$ mm near the piston-mode resonance region, as increased wave steepness can lead to a larger damping effect. The response is overestimated by WAMIT near the resonance region owing to the neglect of viscosity. In non-resonant regions, the WAMIT predictions generally align well with the experimental results.

Fig. 3 (a) illustrates the piston-mode resonance around $T = 1.36$ s and the first longitudinal sloshing response at $T = 0.98$ s under head waves. Additionally, the first diagonal sloshing mode response at $T = 0.68$ s is observed in the white-noise test results. However, this response is not observed in the WAMIT predictions as a result of the symmetric configuration under head waves.

As illustrated in Fig. 3 (b), the first longitudinal sloshing mode ($T = 0.98$ s) is not observed at WG3, as WG3 is located at the center of the moonpool. Fig. 3 (c) shows that the free-surface responses at WG5 and WG10 inside RMP0 are nearly the same in amplitude under a head wave condition. Fig. 3 (d) shows that the response amplitude of white-noise tests at WG1 caused by the piston mode is smaller under beam waves than under head waves. Furthermore, as shown in Fig. 3 (d)-(f), a hump appears ($T \sim 2.3$ s) in the moonpool response, which can be attributed to roll resonance under beam waves.

Fig. 4 presents the motion responses of the ship with RMP0 under head and beam waves. In Fig. 4 (a), the first longitudinal sloshing mode ($T = 0.98$ s) generates a peak in surge RAOs under head waves, whereas the piston-mode resonance ($T = 1.36$ s) has a negligible effect on surge motion. Fig. 4 (b) shows that the piston-mode resonance noticeably amplifies the heave response compared to the NMP case. As depicted in Fig. 4 (c), the piston-mode resonance only slightly influences the pitch motion, since RMP0 is located near the center of the ship. Fig. 4 (d) shows that the first transverse sloshing mode ($T = 0.69$ s) induces motion responses of sway under beam waves. Fig. 4 (e) shows that the piston mode slightly decreases the heave response under beam waves, contrasting with its obvious effect under head waves and highlighting the influence of wave direction on the coupled response of the ship and the clean moonpool. Fig. 4 (f) illustrates that WAMIT significantly overestimates the roll response amplitude near the natural period of 2.31 s.

Fig. 5 shows the free-surface RAOs at the WGs inside RMP4, along with the motion RAOs of surge, heave and pitch under head waves. Comparing Fig. 3 (a) and Fig. 5 (a), it can be seen that the piston-mode period of RMP4 is longer than that of RMP0, whereas the sloshing-mode periods for RMP0 and RMP4 remain nearly identical. As shown in panel (a), near the piston-mode resonance, the responses of RMP4 under regular waves are lower than those under white-noise tests ($H_s = 80$ mm), due to increased viscous damping. In contrast, the

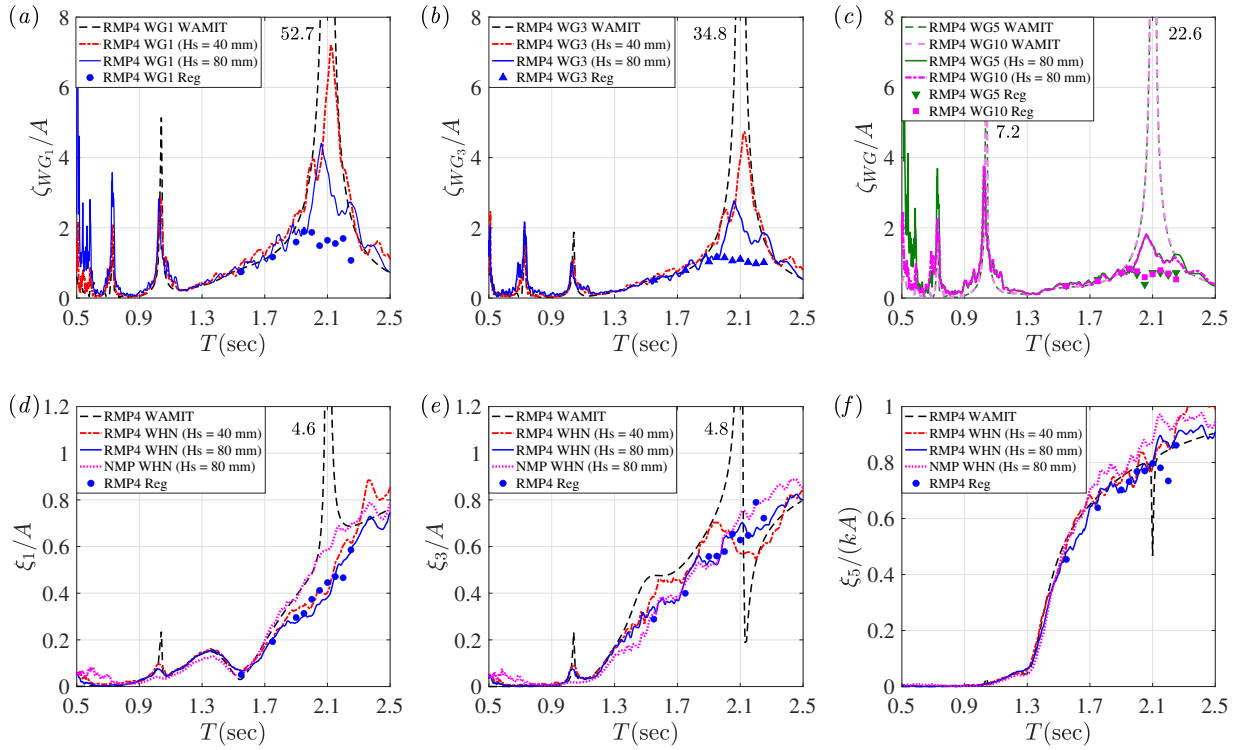

Figure 5: RMP4, motion RAOs of the ship and free-surface response RAOs at different WGs in head wave: (a) WG1; (b) WG3; (c) WG5 and WG10. (d) Surge; (e) Heave; (f) Pitch.

responses of RMP0 under regular waves closely match those of white-noise tests ($H_s = 80$ mm). This difference between RMP4 and RMP0 arises because RMP4 has additional recess edge compared to RMP0, which could cause flow separation and enhance viscous damping.

Unlike RMP0, the first longitudinal sloshing mode ($T = 0.98$ s) with WG3 is observed in Fig. 5 (b), indicating the effects of recess on the modal shape. Comparing panels (a) and (c) in Fig. 5, the free-surface response at WG5 is observed to be smaller than at WG1, which aligns with the piston-mode modal shape with RMP4 of the white-noise tests.

Regarding the motion responses, the experimental results in Fig. 5 (d) show that the piston mode ($T = 2.08$ s) produces a dip in the surge response, which is not observed in RMP0, due to the presence of the recess. In Fig. 5 (e), the experimental results of heave responses are compared with the corresponding WAMIT calculations. This comparison indicates that the effect of piston-mode resonance on heave motion is suppressed due to viscous damping, resulting in only a small hump in the experimental results near $T = 1.92$ s. While the heave response of the ship with RMP0 exhibits a pronounced peak near the piston-mode resonance. Furthermore, the WAMIT results in Fig. 5 (f) indicate that the piston-mode resonance causes a reduction in pitch response. However, this effect is almost negligible in the experimental results, owing to viscous damping. A more detailed analysis will be presented at the workshop.

Acknowledgments

The present work is sponsored by the National Natural Science Foundation of China under Grant No. 52171269.

References

Molin, B. 2001 On the piston and sloshing modes in moonpools. *J. Fluid Mech.* **430**, 27–50.

Molin, B. 2017 On natural modes in moonpools with recesses. *Appl. Ocean Res.* **67**, 1–8.

Molin, B., Zhang, X., Huang, H. & Remy, F. 2018 On natural modes in moonpools and gaps in finite depth. *J. Fluid Mech.* **873**, 571–586.

Senthuran, R., Kristiansen, T., Molin, B. & Ommani, B. 2020 Coupled vessel and moonpool responses in regular and irregular waves. *Appl. Ocean Res.* **96**, 102010.

Zhang, X., Huang, H. & Song, X. 2019 On natural frequencies and modal shapes in two-dimensional asymmetric and symmetric moonpools in finite water depth. *Appl. Ocean Res.* **82**, 117–129.

Zhang, X. & Li, Z. 2022 Natural frequencies and modal shapes of three-dimensional moonpool with recess in infinite-depth and finite-depth waters. *Appl. Ocean Res.* **118**, 102921.

Zhang, X., Yao, J., Beck, R. F. & Bingham, H. B. 2026 The effect of a recess on the nonlinear free-surface responses of three-dimensional moonpools. *J. Fluid Mech.* In press.